Mobile Robots with Novel Environmental Sensors for Inspection of Disaster Sites with Low Visibility

Grant agreement no: 645101

Project start: January 1, 2015

Duration: 3.5 years

Deliverable 2.5

Signal processing algorithms for high-bandwidth chemical sensors

Due date: Month 24

Lead beneficiary: UWAR

Dissemination Level: Public

Main Authors:

Prof. Julian Gardner (UWAR)
Dr. Marina Cole (UWAR)
Mr. Timothy Vincent (UWAR)
Miss. Yuxin Xing (UWAR)

Version History:

0.1: Drafted December 2016
0.2: Submitted January 2017
0.3 Revised February 2017

Contents

1. Introduction and purpose of this report 4
2. MOX Sensor Signal Processing 5
3. NDIR Sensor Signal Processing 10
4. SMR Sensor Signal Processing 15
5. Signal Processing Conclusions 20
6. References 21

1. Introduction and purpose of this report

In the diverse and hazardous environments in which a mobile robot might be deployed, the gas sensor module must be capable of robust functionality regardless of changes in the harsh ambient conditions. Work package 2 (WP2) in the Smokebot project covers the development of *high-bandwidth* (HBW) sensors to identify and map gases found in the environment. Specifically, this document details the development of signal processing algorithms to extract the response to a target analyte in a faster time. The algorithms mitigate the effect of temperature and humidity variation whilst enhancing the response time from the HBW sensors. It is the approach being studied to create higher band-width sensors; it has been applied to MOX gas sensors and NDIR optical gas sensors with a new design of SMR device. The signal processing algorithms can be applied to other gas sensors to enhance their band-width, so it is a generic and powerful approach.

This deliverable addresses Task 2.2, demonstrating the signal processing algorithms tailored for the application of mobile robot gas sensing. The algorithms focus on the state-of-the-art HBW sensors developed at UWAR, with signal processing demonstrated for the CMOS metal oxide (MOX) resistive gas, optical non-dispersive infra-red (NDIR) and solidly mounted resonator (SMR) devices. The advanced signal processing has been demonstrated to improve the detection performance of carbon monoxide (CO), carbon dioxide (CO_2) and toluene, using MOX, NDIR and SMR devices, respectively.

The processing techniques discussed in this report complement the deliverables previous submitted for the Smokebot project.

- Deliverable 2.1 – The technical specification for the HBW chemical sensors.
- Deliverable 2.2 – Characterisation of the HBW sensors.
- Deliverable 2.4 – Fabricated sensor and interface circuitry for the HBW sensors.

The post-collection data analysis permits the HBW sensors to operate within the tolerances listed in the technical specification. The preferred method of signal processing, chosen from a range of techniques to meet the needs of mobile robot sensing, is reported for each of the three sensor types (MOX, NDIR and SMR).

2. MOX Sensor Signal Processing

Two custom MOX (metal oxide) resistive CMOS-based gas sensors are housed inside the gas sensing unit for the detection of CO and NO_2, respectively. When a sensor is exposed to the target gas, the reaction between chemisorbed oxygen ions in metal oxide and the gas creates electrons that reduces the depletion region, thus enhances inter-granular carrier mobility, reduces the sensor resistance and changes the output voltage. Although MOX sensor has a relatively fast response for chemical sensors, it takes seconds to come to steady state, and seconds to recover fully back to the baseline. In order to reduce the response time to under 1 second, a temperature modulation technique is adopted here. Because the MOX sensor operates on a micro-hotplate, it is sensitive to temperature changes. The operating temperature of the micro-hotplate is controlled and altered through pulses of input voltages that are sent from a microcontroller PWM output. But to demonstrate this technique, the sensor is controlled through a data acquisition system (DAQ) by National Instruments. The process method is presented in the flow chart in Fig 1.

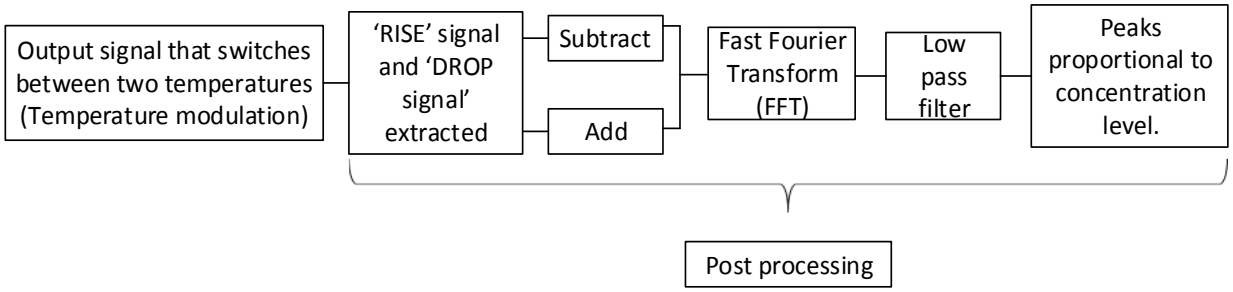

Fig.1: Flow chart for MOX data processing method

The sensor used in the test is the CCS301 chip fabricated by Cambridge CMOS Sensor Ltd (now called AMS UK Sensors Ltd). It has the optimum operating temperature between 200°C and 350°C. According to datasheet, the micro-hotplate temperature has a close to linear relation with the input voltages. So pulses between 0.205 V (OFF) and 0.220 V (ON) are sent to alter the temperature between 250°C and 300°C. Each pulse has a period of 20 seconds with 10 s in each state. Five pulses are sent in total for five cycles, which can be used for averaging later. The sampling rate is set to 100 Hz. SnO_2 based MOX is used for CO detection, and a 300 ppm bottle of CO gas in air is connected. Different concentration levels are explored, as well as in both dry and wet air.

The data are collected through a NI DAQ (USB-6343) as shown in Fig. 2 below. The 'OFF' stage is 0.205V (250°C) and the 'ON' stage is 0.220V (300°C). Each cycle contains 'OFF'-'ON'-'OFF' stages, and the 'OFF-ON' and 'ON-OFF' stages will be used for comparing and analysing.

Both resistance and conductance can be used in temperature modulation; they are calculated based on

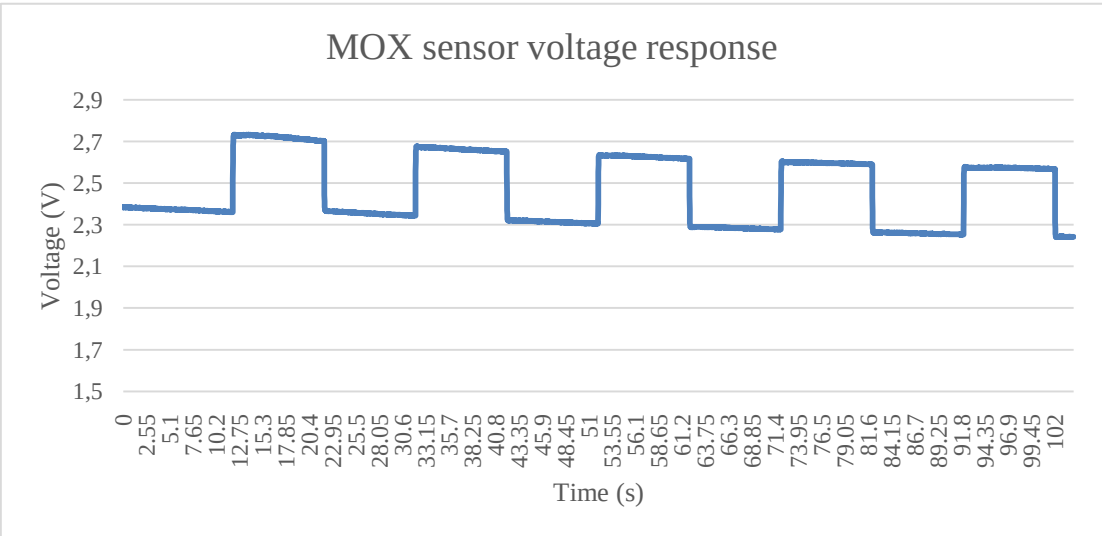

the voltage data collected. The sensor acts as part of a potential divider circuit with selection of load resistance at 1 kΩ, 10 kΩ, 100 kΩ and 1 MΩ. A 1 kΩ load resistor is connected in this test. Details of the MOX circuitry are explained in the Deliverable 2.4.

Fig. 2: SnO_2 MOX raw signal in voltages between 250°C and 300 °C for five cycles in dry zero air

The technique involves subtracting the 'ON' and 'OFF' transient of the resistance signal, and then removing the steady state resistance signal. The rising/dropping moment, t_o, is matched as shows in Fig. 3a). Then one of the graph will be flipped and subtracted to get the difference plot. The linear drift shows in Fig. 2 is removed by using the 'detrend' function provided by MATLAB. The final step is to remove the steady state resistance signal through subtraction to get the plot shows in Fig. 3b).

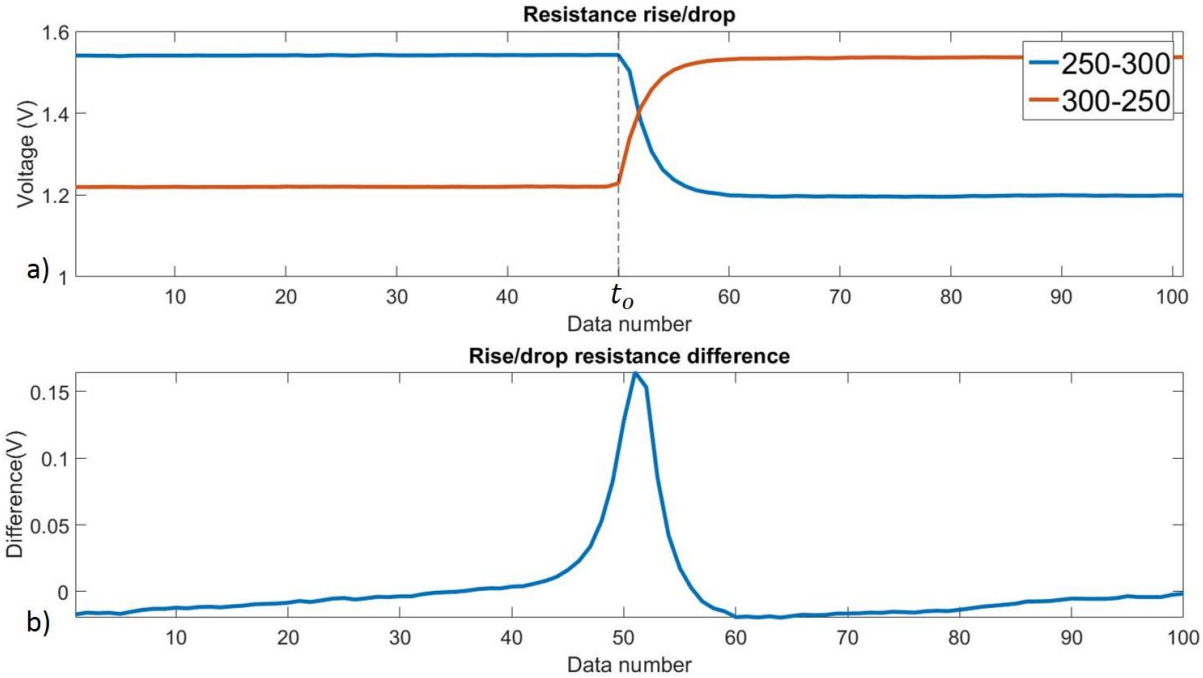

Fig. 3: Temperature modulation using resistance signal in zero air, a) rising and falling plot aligned at t_o , b) resistance difference after normalising.

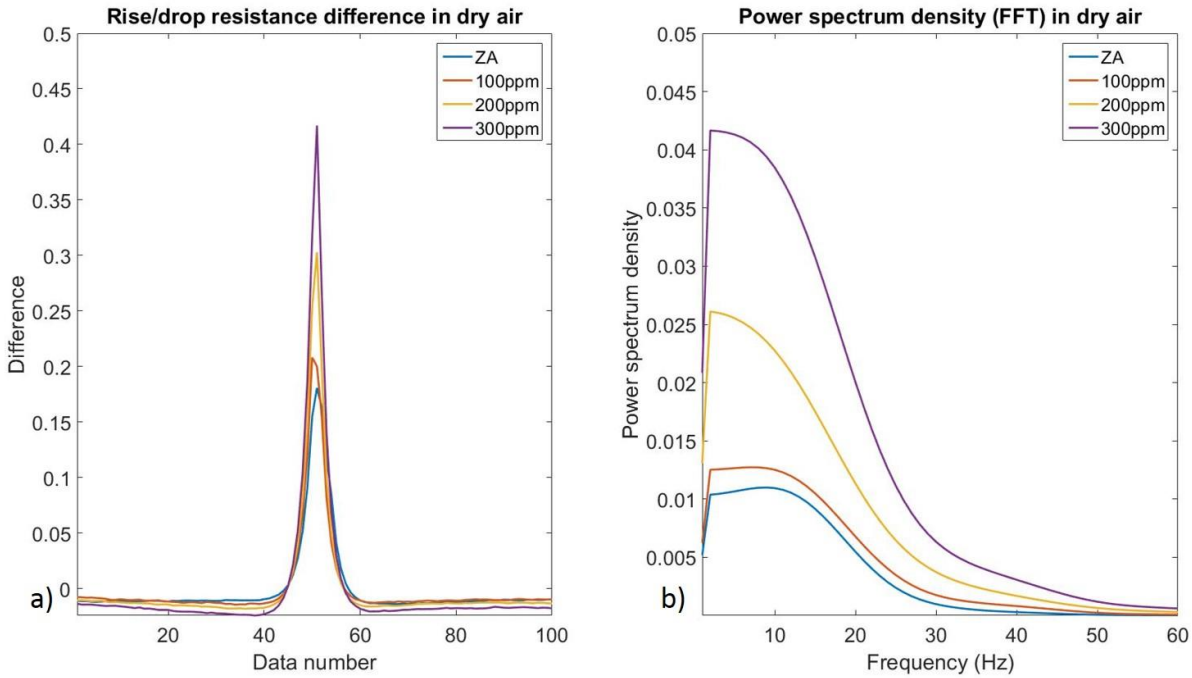

Fig. 4: a) Peaks of resistance difference in dry air in zero air, 100 ppm CO, 200 ppm CO and 300 ppm CO, b) Corresponding FFT power spectrum density plot with low pass filter in dry air in zero air, 100 ppm CO, 200 ppm CO and 300 ppm CO.

The same process is applied to signals collected at different concentration levels: zero air, 100 ppm, 200 ppm and 300 ppm in dry air. Results are shown in Fig. 4. A Fast Fourier Transform (FFT) is then applied to the peak window as well as a low pass filter to get the results shown in Fig. 4b). The peaks are linearly proportional to the concentration levels, which can be used as quicker and better way to identify sensor response and gas concentration level.

Because SnO_2 based MOX is sensitive in humid environment, 15% humidity in introduced. Fig. 5 shows the result in wet air using same modulation method and steps.

Similar to using the resistance signal, the conductance could also be used as an approach for temperature modulation [1, 2]. The only difference is instead of subtracting the 'ON' and 'OFF' transient; they will be summed up as shown in Fig. 6. Same as before, the rising/dropping moment, t_o, is matched before summing. The summed peak signals at difference concentration level are plotted in the same graph for comparison (Fig. 7). The result also presents the linear proportion between concentration level and peak height.

In this section, temperature modulation technique is explored, and SnO_2 based MOX sensor is tested using this method. Temperature modulation is a signal processing technique that can greatly reduce the MOX sensor response time to under a second by rapidly pulsing the micro-hotplate at different temperatures. The maths behind is simple, either subtracting (for resistance) or summing (for conductance) the 'ON' and 'OFF' transient, and then remove the resistance/conductance signal to reveal the peaks. Because of the linear proportionality between gas concentration and peak height, it is a great way to identity sensor response and concentration level, and it will provide detailed information for further gas mapping.

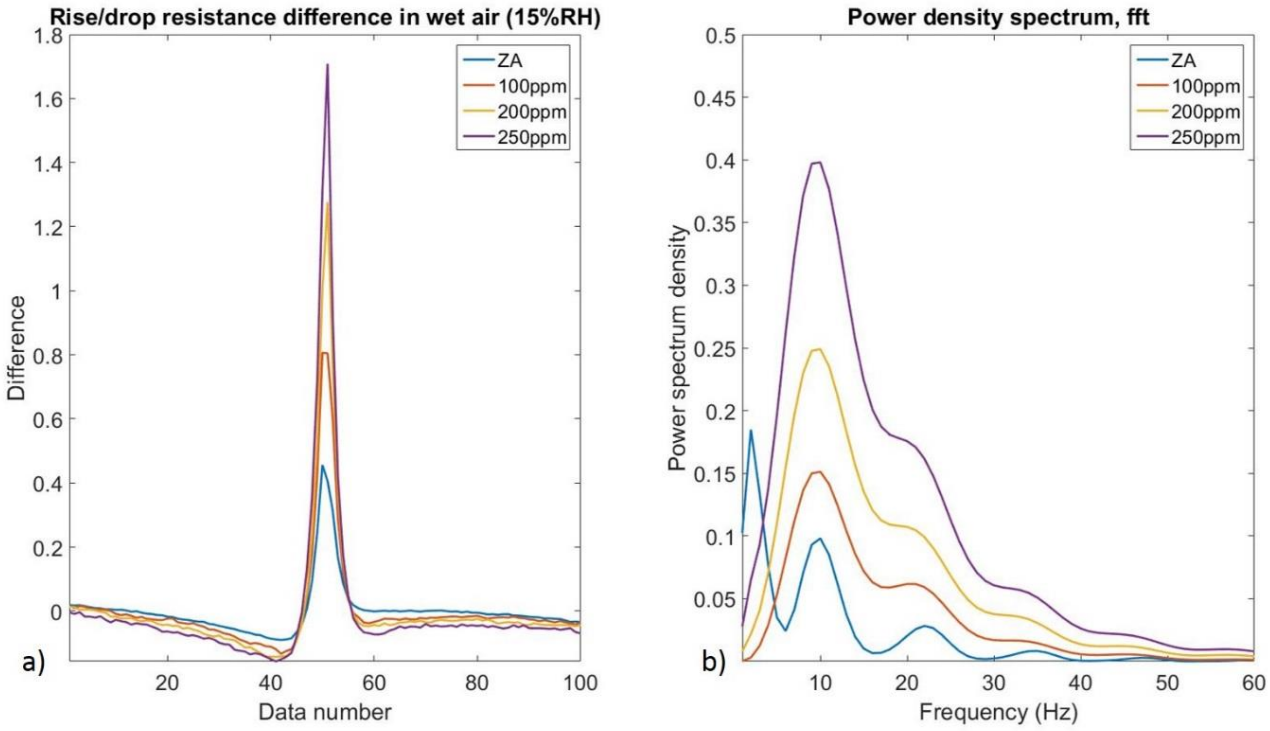

Fig. 5: a) Peaks of resistance difference in wet air (15%RH) in zero air, 100 ppm CO, 200 ppm CO and 300 ppm CO, b) Corresponding FFT power spectrum density plot with low pass filter in wet air (15%) in zero air, 100 ppm CO, 200 ppm CO and 300 ppm CO.

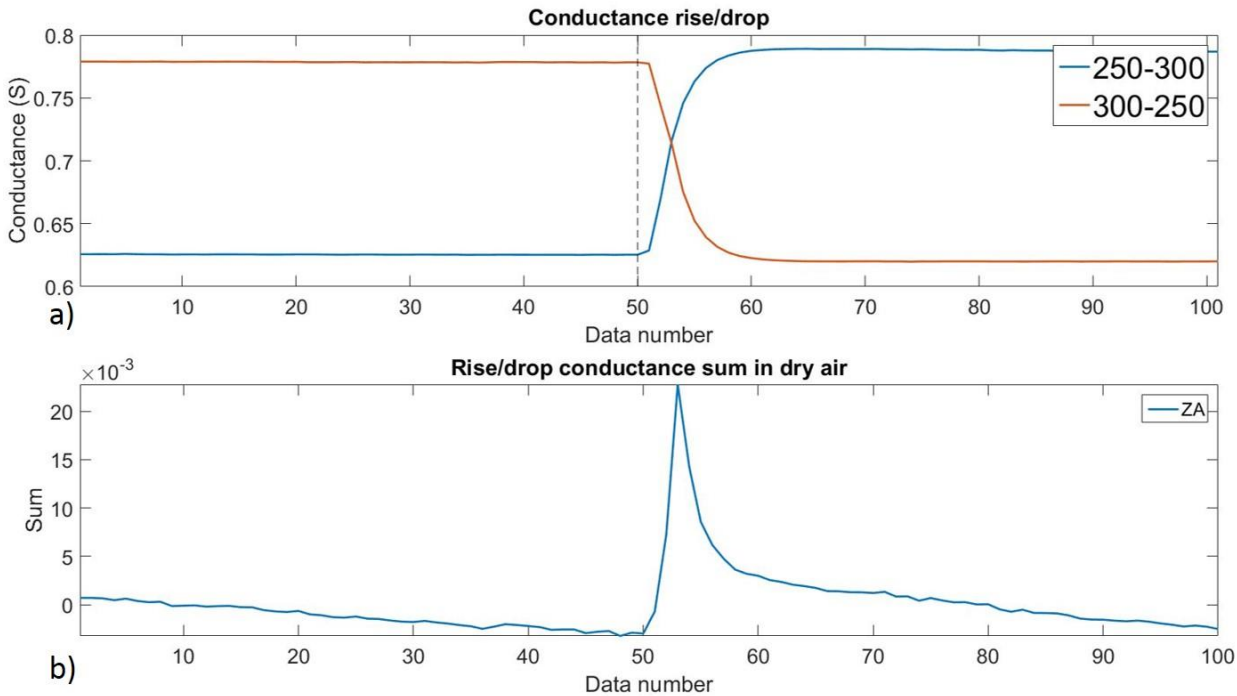

Fig. 6: Temperature modulation using conductance signal in zero air, a) rising and falling plot aligned at t_o , b) conductance sum after normalising.

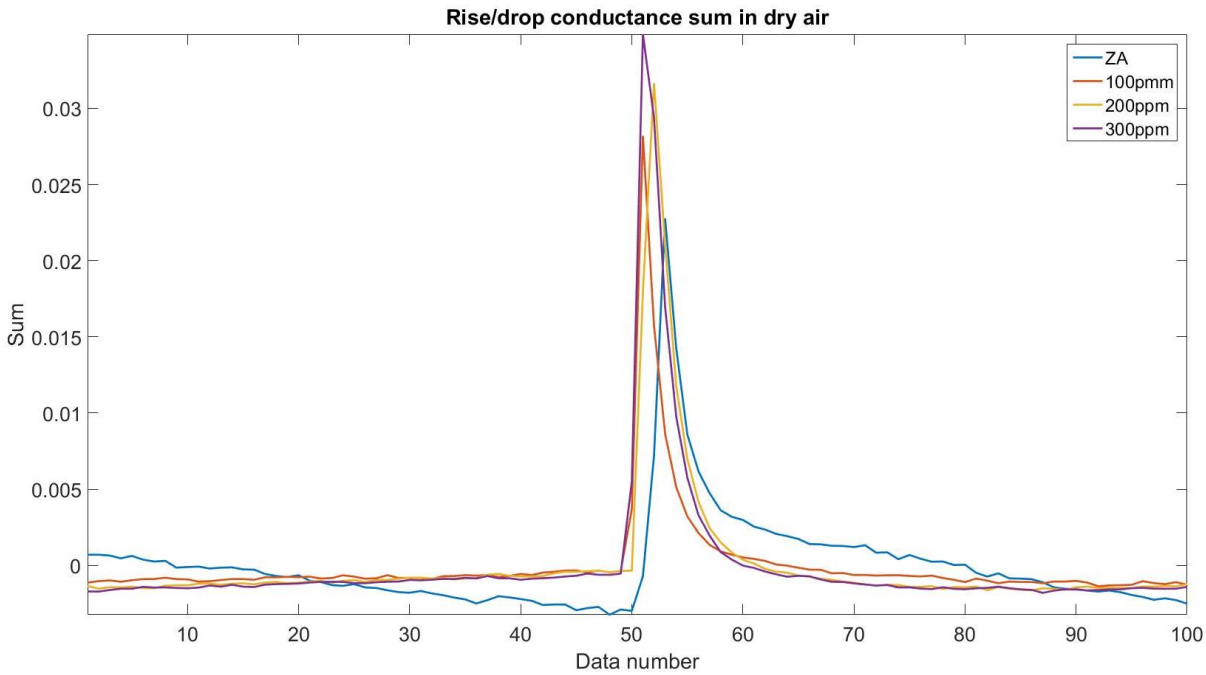

Fig. 7: Peaks of conductance sum in dry air for: zero air, and 100 ppm CO, 200 ppm CO and 300 ppm CO in air.

3. NDIR Sensor Signal Processing

NDIR sensors are classified as physical sensors and detect the presence of a gas by the absorption of infrared radiation by gas molecules. This process occurs almost instantaneously and thus fundamentally NDIR sensors are candidates for fast-response sensor systems. Optical filters can be used to refine the selectivity of the device to a specific gas, for example, CO_2 absorbs light with a wavelength of approximately 4.3 µm. These filters somewhat reduce the cross-sensitivity to humidity and temperature variance, without compromising response time.

The NDIR module developed for the Smokebot project consists of a NDIR emitter (with enhanced emissivity for CO_2 detection) and a dual detector (with the sensing channel filtered for CO_2 detection and the reference at a close wavelength). The subtraction of the reference signal from the sensing channel, in the ideal case, will provide the response to change in CO_2 concentration alone. However, both channels are susceptible to noise pick-up, for example 1/f noise, which is unlikely to be in-phase. The result of the comparison between the signals from the two channels can therefore result in a decrease signal to noise ratio, as the noise present in both channels is summed. Fig.8 a) shows the signal recorded by each channel of a dual detector system with concentrations of CO_2 in the range of 500 to 10 ppm (1 min steps). Fig. 8 b) demonstrates the loss of a clear step between gas concentration changes, as noise is added between the sensing and reference channels.

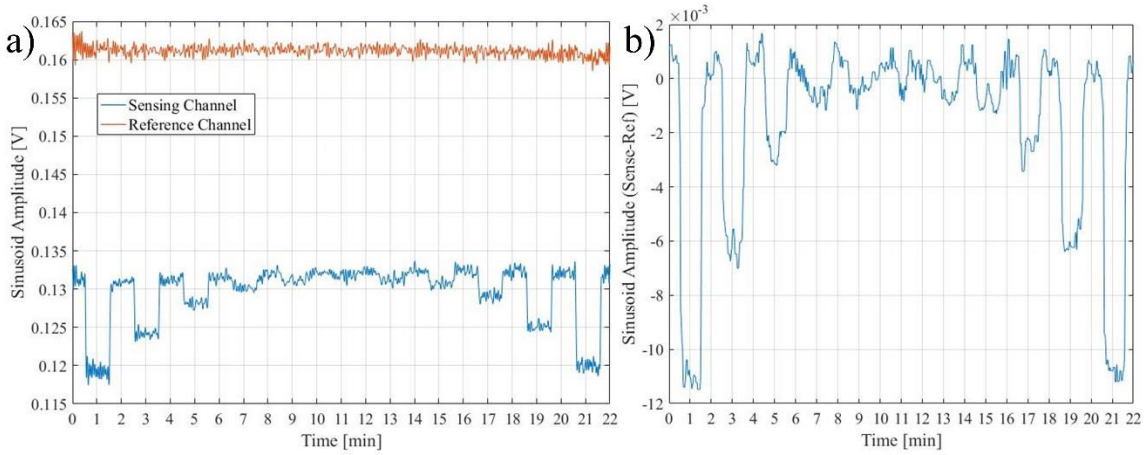

Fig. 8 – CO_2 sensor response to step changes in gas concentration from 500 to 10 ppm, a) Sensing and Reference channels; b) Result of subtracting reference from sensing signal.

The undesired variation in NDIR sensor response (an unstable output) can be avoided using signal processing techniques. In this work, a Fast-Fourier Transform (FFT) is taken of the output NDIR signal as part of a digital filtering process. This method effectively reduces the noise present on the output signal, while maintaining a fast response time without introducing lag through the use of analogue or averaging filtering techniques. The details of this method are shown in the flow chart in Fig 9.

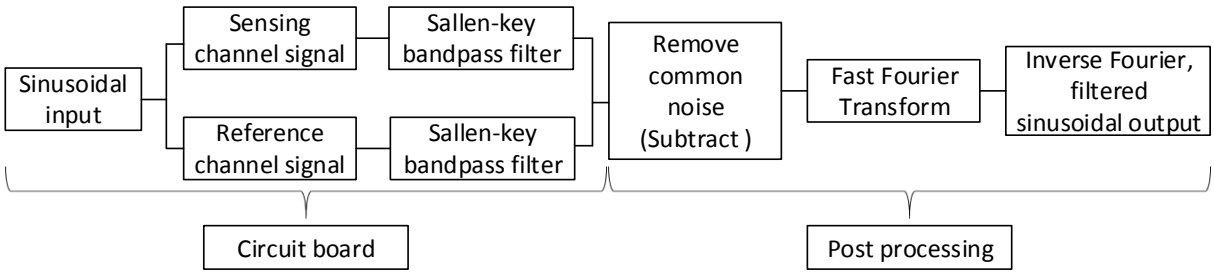

Fig. 9: Flow chart for the NDIR sensor data processing method

A sinusoidal drive signal is preferred for the emitter, which enables the FFT method to be implemented and also reduces the power consumption of the system. Higher frequency drive signals are desired (to increase the read-out rate of the sensor), but the size of the micro hotplate emitter in its current generation limits restricts the frequency to the low Hz range.

Alternatively, a lock-in amplifier can help recover the desired response to CO_2 from the noisy detector output. The amplifier takes an input baseline signal (i.e. the drive signal from the emitter) and compares it to the noisy signal (i.e. from the detector). The frequency present on the input baseline signal is extracted from the noisy signal. The amplitude of the resulting waveform can be used to find the concentration of CO_2 present. Further details of this work have been previously reported [3].

The sinusoidal drive signal oscillates between two temperatures at a frequency of 20 Hz. Fig. 10 a) shows the emitter drive signal, created by a signal generator). The corresponding temperature emitted (from the hotplate) is shown in Fig. 10 b). The sinusoid signal is received at the detector; the amplitude of the sinusoid (magnitude of the FFT) is recorded as the response to the presence of the target gas.

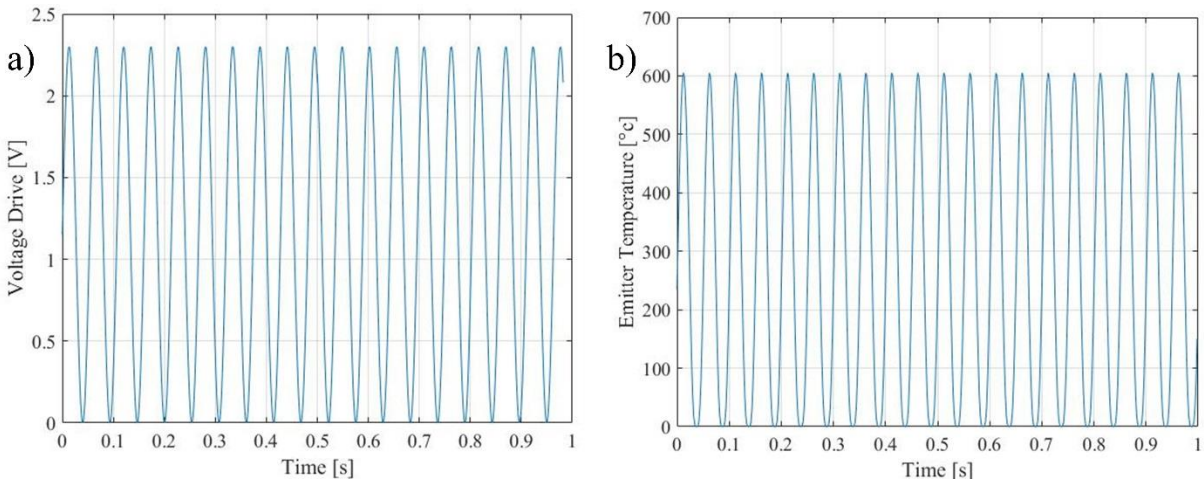

Fig. 10 – Emitter drive signal, a) Voltage output from signal generator; b) 20 Hz sinusoid used to drive micro hotplate, plot shows corresponding temperature emitted.

Fig. 11 shows the output signal from the detector, without any filtering. The concentrations of CO_2 under test are shown. Each concentration was tested for 1 min step, returning to a baseline of synthetic air (0 ppm CO_2). The high level of noise on the signal prevents the concentration steps from being visibly distinguished from the baseline output level.

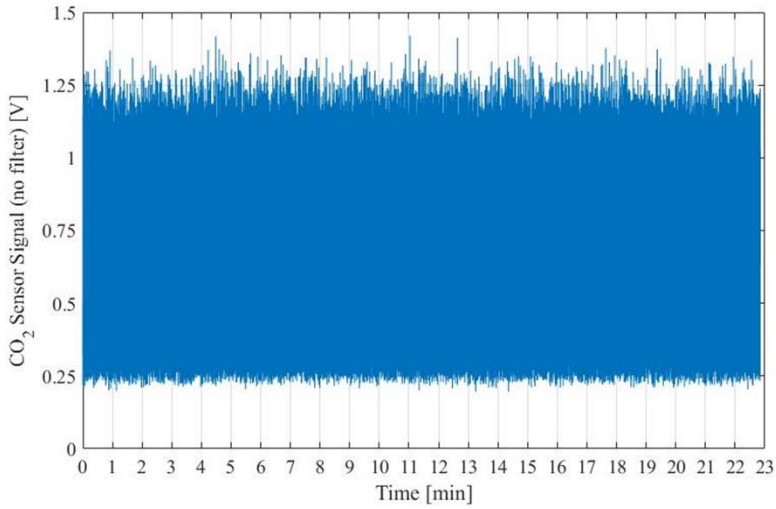

Time [min]	Concentration CO_2 [ppm]
Baseline	0
1	500
3	200
5	100
7	50
9	25
11	10
13	25
15	50
17	100
19	200
21	500

Fig. 11 – Output response from sensing channel of NDIR detector when exposed to concentrations of CO_2 in the range of 10 to 500 ppm.

An analogue bandpass Sallen-Key filter is applied to the raw output from the NDIR detector, centred around 20 Hz. The filtered output is shown in Fig. 12 a). An enlarged view of a 2 s section of the output signal is shown in Fig. 12 b), taken at 60 s into the experiment at the point of a step change from 0 ppm to 500 ppm CO_2. The section shows other frequency components are present in the output waveform in addition to the expected 20 Hz wave. The sinusoidal signal is the dominant component, although the amplitude of the waveform fluctuates, even when a steady baseline is expected.

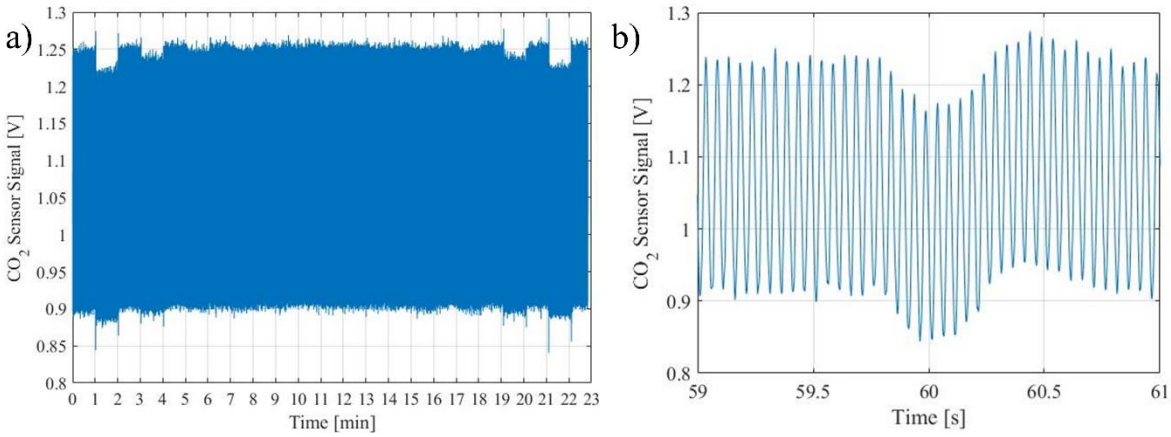

Fig. 12 – Analogue filtering applied to detector signal, b) time series plot of voltage output; b) Enlarged 2 s view of the output, at 60 s into the experiment.

The output response can be recovered from the combination of frequency components through an FFT filtering process. A filter is placed (in the frequency domain) at the frequency of the sinusoid drive signal (20 Hz) and the first harmonic (40 Hz), as shown in Fig. 13 a). These frequencies are passed, whereas the components at all other frequencies are blocked. The amplitude of the resulting sinusoidal waveform to find the change in output of the sensor due to the varying concentrations of CO_2. This output response is shown in Fig. 13 b).

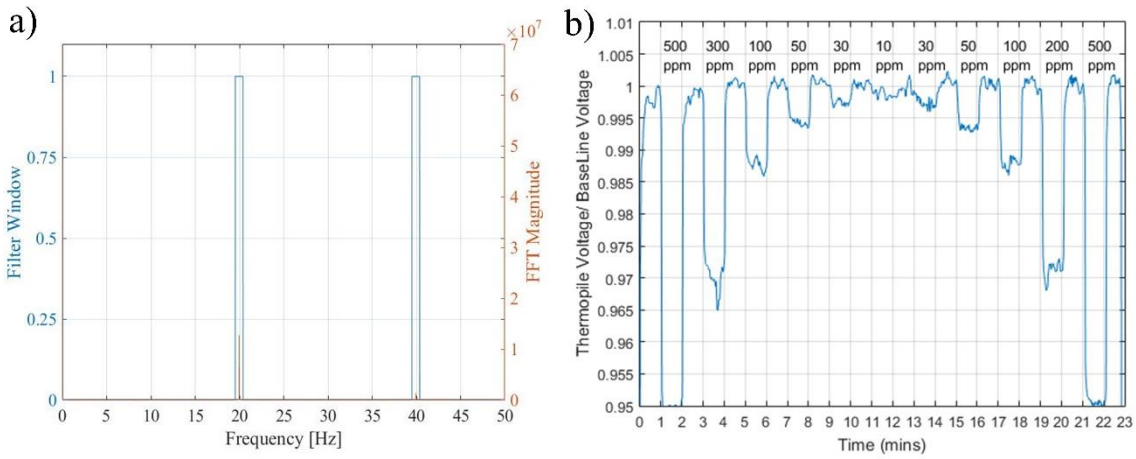

Fig. 13 – FFT filtering process, a) Only desired frequency and one harmonic passed to remove noise at other frequencies; b) Amplitude of sinusoid taken from FFT filtered signal.

In the data presented above, the concentrations are in the low ppm range up to 500 ppm. The limit of detection of the sensor is in the low ppm range (when an optical path of 8 cm is used). The output responses exhibit reduced levels of noise after the filtering procedure; however deterioration of the output signal is notable at concentrations < 50 ppm.

The level of filtering that can be applied is limited by the drive frequency. To avoid compromising response time, no median or moving average filters were applied. Such filters help reduce the jitter present on the output which can be added from external sources or during the data acquisition process. Work is ongoing to develop devices which can operate at higher frequencies to enhance the available filtering methods. The sensors can also be optimised for the detection of a desired gas. The emissivity of the emitter can be enhanced at a wavelength at which the gas molecules are absorbed, while avoiding the wavelengths of which other molecules (e.g. water vapour) cause interference.

The FFT filtering method is effective at removing drift caused by the IR emitter stabilising. This can occur if limited time is available for the device to stabilise before it is used. In the example shown in Fig. 14, data is recorded immediately after the device is switched on. During the first 5 minutes of its use the recorded output voltage increases, as the system stabilises to temperature. Fig. 14 a) shows the unprocessed output data from the NDIR detector. After the FFT filtering procedure, the output is shown in Fig. 14 b). Although minimal drift is still present, the response to the 1 % step change in CO_2 (at 1.5 and 3.5 min time points) is visible.

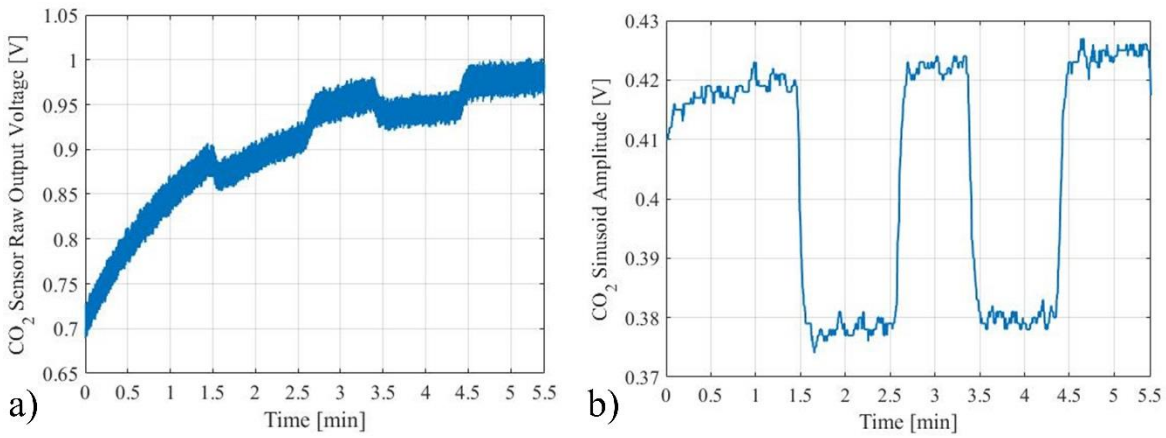

Fig. 14 – Example of start-up drift removal using the FFT filtering method, a) Raw signal output from the NDIR detector; b) Response to 1 % steps in CO_2 visible after data processing.

The variation in environmental temperature can cause an exponential drift, similar to the start-up transients shown in Fig. 14. The FFT filtering method removes the low frequency drift and enables the sensor to operate without requiring temperature regulation. The dual detection configuration further mitigates the risk of environmental factors lessening sensor performance.

This filtering procedure provides excellent performance, however at the cost of computational power. It is essential a narrow window is applied around the 20 Hz peak, in the frequency domain, shown in Fig. 13 a), to ensure the effective removal of noise. In the filtering processes a high number of samples are required (i.e. sampling at 200 Hz or greater) to ensure sufficient samples are collected to be able to choose a narrow window around 20 Hz (i.e. there is a need to be able to distinguish 20 Hz from for instance 21 Hz etc.). It is only with the newest generation of microcontrollers that this method is accessible for use in real-time in mobile applications.

4. SMR Sensor Signal Processing

Acoustic wave based devices are versatile sensors, and can be used in a wide range of applications, for example detection of temperature, humidity, VOCs, gases and particles. Solidly Mounted Resonators (SMRs) consist of a thin piezoelectric layer sandwiched between metal electrodes on top of an acoustic mirror formed by alternating layers of low acoustic and high acoustic impedance materials. These devices are preferred over other acoustic sensors (e.g. quartz crystal microbalance or surface acoustic wave) because the thin film technology allows operation at higher frequencies (e.g. 900 MHz) which in turn enhances sensitivity.

In this work the SMRs were fabricated using zinc oxide as the piezoelectric layer and aluminium electrodes deposited on an acoustic mirror (formed of 3 pairs of Mo/SiO_2 layers). The devices were driven with a Colpitts type oscillator configuration. They were designed to resonate at 900 MHz without any mass loading. A cross-section view of an SMR device is shown in Fig. 15 a), with the fabricated device shown in b). Further details about the devices have previously been reported [4].

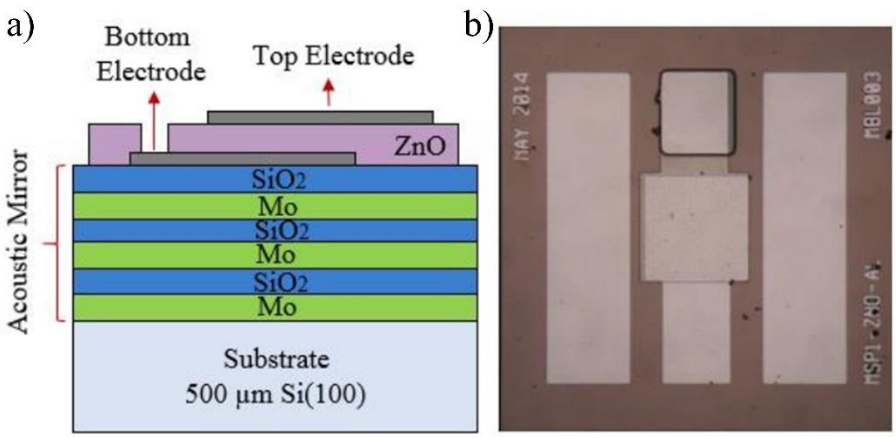

Fig. 15 a) Schematic of the cross-section view of the designed SMR; b) Top view of the fabricated SMR resonating at 900 MHz (1mm x 1 mm dimensions).

SMR sensors can be used for a wide range of applications, thus it is important they are made selective for the desired purpose. In the case of VOC sensing, the sensing area of the devices can be coated with a thin polymer layer. The polymer is selected based on the target gas, for example poly methyl (cyano propyl) sibxane (PMCPS) is particularly suited for the detection of toluene, and fluoroalcohol polysiloxane (SXFA) is used for the detection of acetone. The absorption of the VOC into the polymer layer causes a change in mass, which affects the frequency at which the device resonates. The sensitivity is described by the Sauerbrey equation (1) [5].

$$\Delta f = \frac{2\, f_0^2}{A\sqrt{\rho_q \mu_q}} \Delta m \qquad (1)$$

The Sauerbrey equation demonstrates the initial resonant frequency (f_0) has a significant impact on the magnitude of the frequency shift, thus devices that operate at higher frequencies offer a higher sensitivity. The frequency shift (Δf) is proportional to the mass change (Δm) and inversely proportional to the piezoelectrically active crystal area (A), the density (ρ_q) and the shear modulus (μ_q) of the material. In this work, in mobile robot exploration, fast response sensors are preferred. The thickness of the polymer coating applied to the sensor is inversely proportional to the speed of

response (i.e. a thinner coating is preferred to enable fast reactions inside the layer, and thus a fast sensor response).

The thickness of the coating can be in the range of 100 to 500 nm, depending on the polymer selected and the sensitivity needed. The coating is deposited onto the devices by spraying a 0.5 % w/v (weight/volume percentage) polymer solution onto the surface. An airbrush is used to disperse a thin layer onto the devices, which are mounted on a spinning platform (rotating at ~50 rpm). This method enables a thin coating to be applied evenly across the surface of the devices. Fig. 16 a) shows the SMR after it has been coated. The thickness of the device is measured, as shown in Fig. 16 b), where the red area indicates the coating. The thickness is measured from the bottom of the device in this subplot. Fig. 16 c) shows the thickness measured from the surface of the device. The coating is measured in the z orientation, which in this example, has a thickness of 0.408 µm.

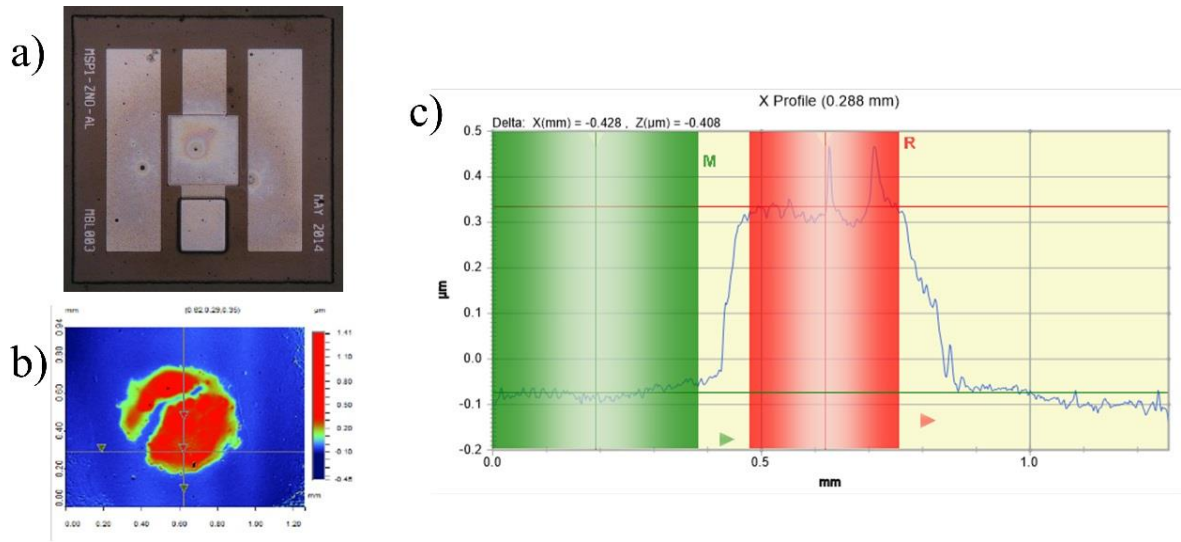

Fig. 16 a) Photograph of coated SMR device (1 mm x 1 mm dimensions); b) Colour map showing the thickness of the device (measurements from bottom of device); c) Thickness profile (z-axis) for the coated layer for the device.

The SMR sensors can be sensitive to external elements, such as humidity, temperature, vibration, flow speed and pressure. To help reduce the effect of these elements on the sensor response to a desired VOC, acoustic sensors are usually operated in differential pairs. A reference device (without any surface coating) is subtracted from a sensing device, coated with a polymer, to remove the interference from any other effects other than the compound of interest (to which the coating is sensitive). To prevent any additional noise being added to the RF signals, this processing is performed using a mixer, which can be located in close proximity to the SMR devices.

The mixer subtracts the signal, and produces an output containing the sum of the differential signals and the subtracted value. A low pass filter is used to remove the unwanted high frequency components, and thus the output is solely the subtracted signal. A comparator is used to convert the sinusoidal signal into a square wave, which can easily be recorded using a microcontroller. See Fig. 17 for the flow chart of this processing method.

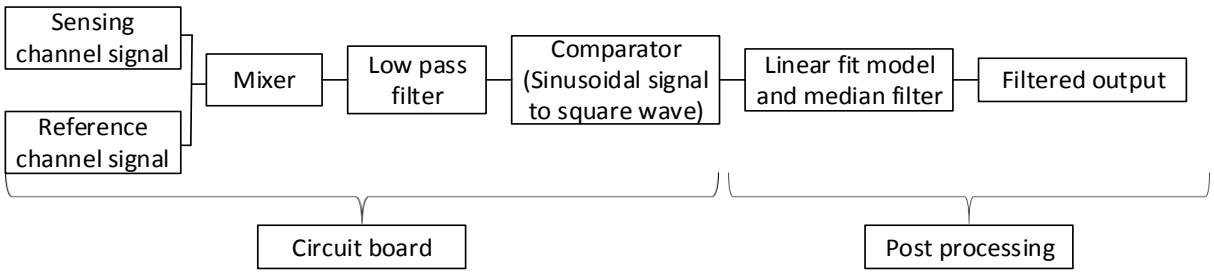

Fig. 17: Flow chart for the SMR data processing method

The output from the system is still susceptible to noise pickup from external sources, or from changes in resonant frequency of the SMR devices. Fig. 18 shows the raw recorded output from an SMR sensor system. The baseline shift drifts, and there are spikes caused by the change in flow rates when a step change in gas concentration is implemented.

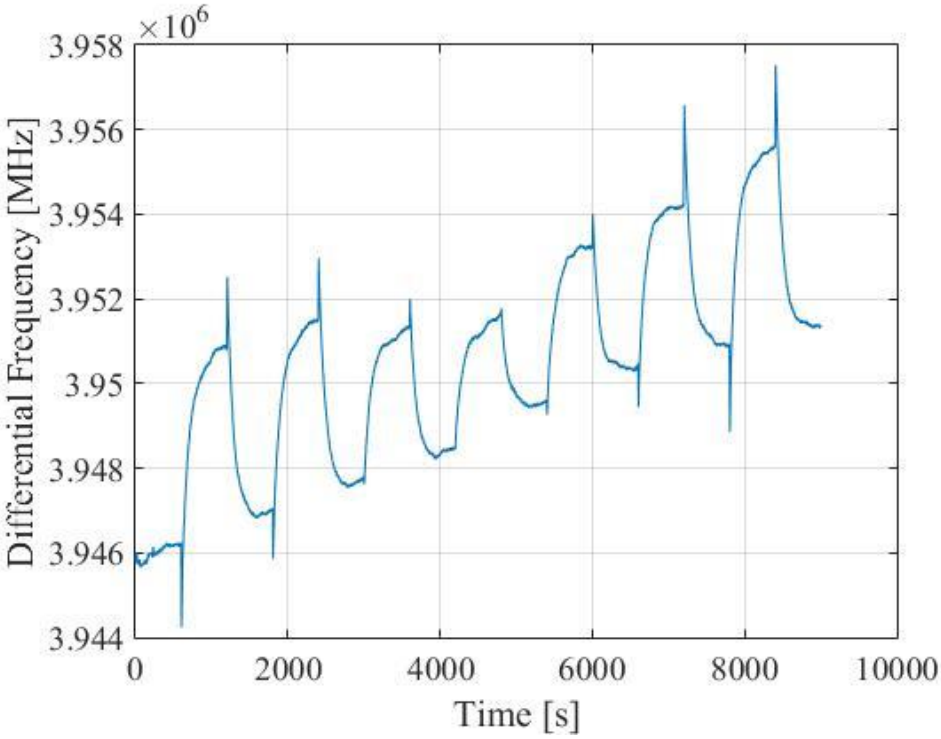

Fig. 18 – Raw differential signal recorded from SMR system using a microcontroller.

The SMR signal is processed in Matlab, to remove the drift on the signal, and to filter the spikes from the change in VOC concentration. The code removes the linear drift which is visible on the raw sensor output. A baseline of 0 Hz shift (when the sensor is in air) is defined. A median filter is applied to reduce the spikes caused by a change in gas flow rate. The resulting output is shown in Fig. 19. In this experiment, the sensor was exposed to between 5 ppm and 75 ppm of toluene. The device was coated with a 100 nm layer of PMCPS. The maximum frequency shift occurs for 75 ppm toluene, where a 4200 Hz shift is observed.

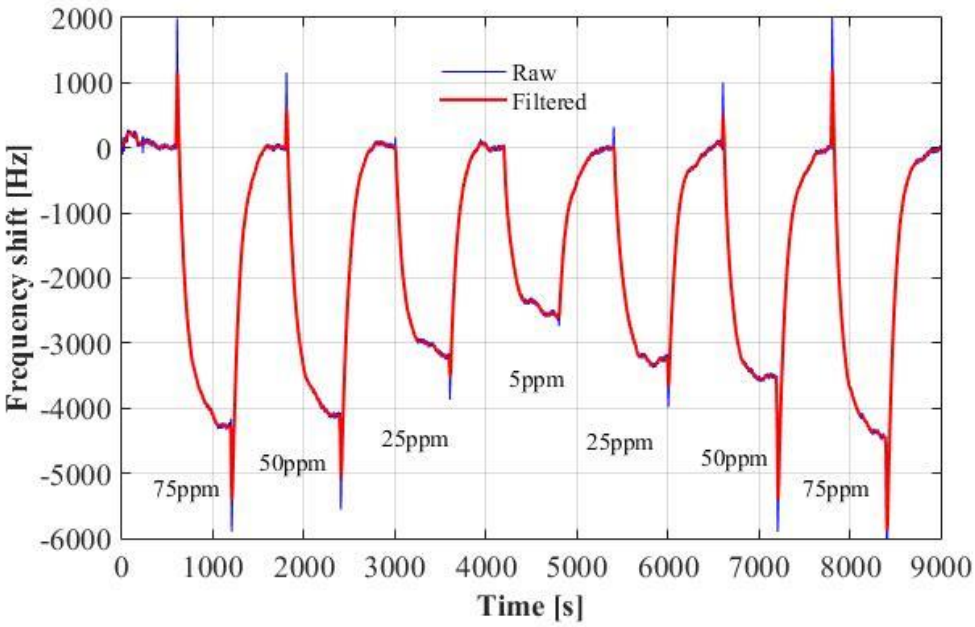

Fig. 19 – SMR sensor output after filtering and linear drift is removed.

A second device was tested to a higher concentration of toluene (between 25 and 100 ppm). The processed device output is shown in Fig. 20. The drift present on the raw output was removed. The sensors used in this experiment (100 nm coating) had a lower cross-sensitivity to gas flow rate changes (this effect can be removed in the case of this experiment).

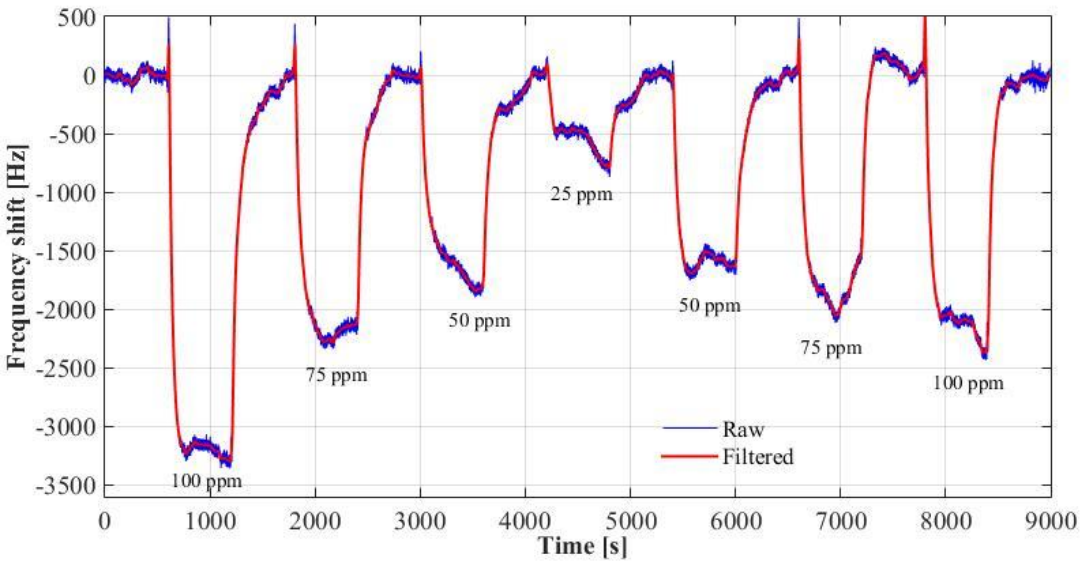

Fig. 20 – SMR sensor output after data processing, showing response to between 25 and 100 ppm of toluene over a period of 9000 s.

The majority of the signal processing for the SMR devices is performed prior to data logging (i.e. a mixer chip is used). When the signal oscillates at 900 MHz, it is necessary to perform some post-processing techniques before the signal can be logged using a microcontroller (as required for the Smokebot project). The mixer subtracts two high frequencies signals, and (after filtering) produces a differential signal. This signal (in the range of 0 to 10 MHz) can be logged using a microcontroller.

The signals can be susceptible to drift, which must be removed in post-processing. A linear fit can reduce the drift present in the SMR sensor experiments. The differential output is further filtered, to reduce the noise present at low frequencies.

The response is still relatively slow and new devices have been designed with integrated heaters that could permit the thermal modulation technique to be applied again.

5. Conclusions

5.1 MOX

The output from resistive MOX gas sensors was modified using an FFT technique. A thermal modulation technique was used to compare the response of the sensors to different gases. A 10 s pulse between 250 and 300 °c was used with a tin oxide coated MOX device. The initial 0.5 s of the pulse was investigated in the frequency domain.

The thermal modulation enabled the effect of the sensor being exposed to a different gas concentration to be investigated in a short time window. The frequency components inside the 0.5 s pulse can be used to determine the type of gas the sensor is exposed to, and the concentration. A relevant gas to the Smokebot project was selected (CO), and concentrations from 100 to 300 ppm were trialled.

The results from the FFT processing technique found it was possible to distinguish the concentration of CO to which the device was exposed, from the 0.5 s window taken from the temperature pulse. Further work could involve testing mixtures of gases and lower concentrations of CO. Of particular interest to the Smokebot project, would be the investigation of how other compounds (smoke, temperature or humidity variation) effect the output from the sensor.

5.2 NDIR

The NDIR sensor system also requires FFT processing to extract the useful information from the noisy received signal. The low sinusoidal frequency drive (20 Hz) limits the post-processing techniques available. A dual channel system is used to help reduce the interference from changes in water vapour or temperature during the experiments.

The raw output from the thermopile used in the CO_2 sensor is plagued with low and high frequency noise, which can only be partially removed using traditional filtering techniques (e.g. a Sallen-key filter). FFT filtering offers the advantages of fast signal processing, without the added time delay caused by high order analogue filters. The FFT is taken of the received signal from the CO_2 thermopile. The magnitude of the FFT result (the amplitude of the received 20 Hz sinusoid) equates to the response to the presence of CO_2 gas.

The FFT filtering technique was demonstrated for gas concentrations in the order of 10 to 500 ppm CO_2. The data is notable cleaned following the processing technique, although some noise is still present at lower concentrations. The technique can also remove low frequency drift, most visible upon initial start-up of the device. The amplitude of the sinusoid drive frequency remains constant if the gas concentration of CO_2 is not varied. Further work for the CO_2 sensor signal processing involves driving the system at a higher frequency. A new generation of IR emitters is being designed and fabricated that will enable much higher drive frequencies and so faster sensor responses. We expect this to enhance the bandwidth further by a factor of at least 5.

5.3 SMR gas sensors

The SMR gas sensor system requires less post-logging signal processing, where a dedicated mixer chip performs a level of signal processing. In the standard differential system, a reference sensor output is subtracted from a sensing signal. This differential signal is filtered, to remove higher frequency components. The result of this processing is logged using a microcontroller.

The sensor system is susceptible to drift, which causes a linear increase in frequency over the course of an experiment. This baseline drift can be removed by using a linear fit method. The signal must also

be filtered to remove spikes caused by change in gas flow or other variables. The sensor system was trialled to toluene concentrations in the range of 5 to 100 ppm.

Further work for the SMR system involves the development of an improved chamber housing to reduce the dependence of the system on flow rate. We are also developing a new SMR chip with an integrated heater (patent pending) which will enable us to modulate the SMR operating temperature and run it above ambient. These methods will again enhance the bandwidth further of our SMR sensor.

6. References

1. T. Iwaki, J. A. Covington, and J. W. Gardner, "Identification of Different Vapors Using a Single Temperature Modulated Polymer Sensor With a Novel Signal Processing Technique," *IEEE Sensors Journal*, vol. 9, pp. 314-328, 2009.
2. T. Iwaki, J. A. Covington, F. Udrea, and J. W. Gardner, "Identification and quantification of different vapours using a single polymer chemoresistor and the novel dual transient temperature modulation technique," *Sensors and Actuators B: Chemical*, vol. 141, pp. 370-380, 9/7/ 2009.
3. T. A. Vincent and J.W. Gardner, “A low cost MEMS based NDIR system for the monitoring of carbon dioxide in breath analysis at ppm levels”, *Sensors and Actuators B: Chemical*, vol. 236, pp. 954-964, 2016.
4. F.H. Villa-Lopez, G. Rughoobur, S. Thomas, A. J. Flewitt, M. Cole and J.W. Gardner, “Design and modelling of solidly mounted resonators for low-cost particle sensing”, *Measurement Science and Technology*, vol. 27, 2016.
5. G. Sauerbrey, “Verwendung von Schwingquarzen zur Wägung dünner Schichten und zur Mikrowägung”, Z. Physics, vol. 155, pp. 206-222, 1959.